J. Membrane Biol. 33, 1–20 (1977)

A Gradient of Diffusible Substance in a Monolayer of Cultured Cells

W. Michalke

Institut für Biologie III der Universität Freiburg, Freiburg, W. Germany

Received 18 February 1975; revised 4 October 1976

Summary. Monolayers of hypoxanthine phosphoribosyl transferase-deficient and their corresponding wildtype cells have been placed adjacent to each other with a newly described method. Autoradiographs from such preparations after incubation with ^{3}H-hypoxanthine allow the direct visualization of gradients of incorporated radioactivity at the border between the two cell types. The gradients can be described by an exponential function, and the amount of radioactivity incorporated decreases to less than 1% at a distance of 1 mm from the wild-type cells. A possible mechanism to convert exponential gradients to linear ones over a certain concentration range is discussed.

Gradients of diffusible substances have been considered as being responsible for the phenomenon of polarity in orderly development of multicellular organs and organisms (Morgan, 1905; Child, 1928; Lawrence, Crick & Munro, 1972). That such gradients do exist and act in the expected manner has still not been proven. It has been pointed out, however, that an ensemble of cells connected by communicative junctions can provide the space, where such gradients could build up without too much interference from the extracellular environment (Loewenstein, 1968*a*, *b*). Gradients of induced intracellular electrical potential have been demonstrated in salivary glands of *Drosophila* larvae (Loewenstein & Kanno, 1964), salivary glands and Malpighian tubules of *Chironomous* larvae (Loewenstein *et al.*, 1965) and mouse liver tissue (Penn, 1966; Loewenstein & Penn, 1967).

The discovery of metabolic cooperation between tissue culture cells (Subak-Sharpe, Bürk & Pitts, 1966) has offered the possibility of measuring the transfer of diffusible substances from cell to cell without the aid of electrical measurements, provided a mutant blocked in the metabolism of an easily traceable molecule is available. In such a system

containing mutants, that are unable to incorporate radioactive hypoxanthine into nucleic acids by themselves (IPP^-), gradients of hypoxanthine-derived radioactivity have been observed occasionally in a few consecutive mutant cells connected to one wildtype cell (Subak-Sharpe, Bürk & Pitts, 1969). Metabolic cooperation appears also to depend on communicative junctions, since it cannot be detected in cells in which these are lacking (Azarnia, Michalke & Loewenstein, 1972; Gilula, Reeves & Steinbach, 1972). In this paper a method is described which allows direct visualization of a gradient of diffusible substance, using metabolic cooperation in a monolayer of epithelioid cells. A few examples of gradients are demonstrated, and a mechanism is proposed for converting the obtained exponential gradients into almost linear ones for a concentration range of two orders of magnitude. This mechanism might operate in natural cell populations.

Materials and Methods

Cells

The following cells have been used. Rat liver epithelial cells (RLB) (Borek, Higashino & Loewenstein, 1969); a hypoxanthine phosphoribosyl transferase (HPRT) negative mutant of RLB (RLB $HPRT^-$) isolated by U. Friedrich in this laboratory; rabbit lens epithelial cells (lens) (Shapiro *et al.*, 1969).

Media and Culture Conditions

Modified medium F12 was prepared according to Ham (1972). It was used supplemented with 10% fetal calf serum (Grand Island Biological Corporation) for subcultivation of cell lines as well as for experiments. When labelling with radioactive hypoxanthine (Amersham Buchler) was required, the concentration of nonradioactive hypoxanthine added to the medium was reduced at least one day before the experiment to 10^{-7} M or to 10^{-6} M. These are both lower concentrations than that of the added radioactive hypoxanthine.

For subcultivation and experiments, the cells were incubated in surface coated plastic Petri dishes (Greiner, Nürtingen) at 37 °C and equilibrated at pH 7.3 in a CO_2-air mixture of 95% relative humidity.

Arrangement of Cells for Transfer Experiments

Two or more different cell types were seeded into four wells on a 5 cm plastic petri dish. The wells were formed with the aid of a flat piece of plastic (Sylgard 184, Dow Chemicals) placed on the bottom of the petri dish. Four square holes of approximately 50 mm^2 size were cut into the plastic with a piece of razor blade, leaving a thin (0.4–0.8 mm) plastic cross bar which separated the four holes. The silicone plastic bars adhered well enough in most cases to separate the four compartments completely. Leaky preparations,

as judged from the microscopical observation of more than one cell type per compartment or by the appearance of cells underneath the silicone, were not used. The cells seeded into the different compartments were allowed separately to adhere to the bottom of the dish overnight. They were then rinsed gently with phosphate buffered saline and the Petri dish was filled with enough medium F12 to cover the silicone piece (at least 5 ml). In this condition the cells were allowed to grow until a dense monolayer was formed. No multilayering occured with any of the cell lines used. After careful removal of the silicone piece, the cells at the new free edge started to crawl into the free space and to proliferate, and came into contact with cells from the neighboring compartment after 10–20 hr, depending on the size of the separation zone. Two or four days after the first contact formation ^{3}H-hypoxanthine was added at 1 μCi/ml (specific activity 570 mCi/mmole), and the cultures incubated overnight (16–24 hr).

Fixation and Autoradiography

At the end of an incubation period, the cells were rinsed twice with 5 ml of phosphate-buffered saline (PBS) and incubated for an additional 30 min in F12. Rinsing with PBS was then repeated and the cells were fixed overnight with 0.5% glutaraldehyde in PBS at 4 °C. The fixed cells were rinsed several times with tap water, ice-cold trochloracetic acid, and distilled water and were air dried thereafter. The dry dishes were covered with a film from a 1:1 mixture of water and nuclear track emulsion NTB-3 (Kodak). After exposure for one week or more, the film was developed with D19 (Kodak) for 3 min, rinsed with tap water and fixed for 4 min and rinsed again with tap water for 10 min and air dried.

Staining and Observation of the Preparations

The cells in the dried dishes were stained with a 1:15 dilution of Giemsa's azur-eosin-methyleneblue solution in distilled water, rinsed, air dried and covered with coverslips for microscopical observation. Photographs from the border region between neighboring compartments were taken with a Ultraphot II Photomicroscope (Zeiss). Bright-field illumination was used to distinguish cell types, whereas dark-field illumination on the same region was used to show the silver grains only.

The silver grains of the dark-field photographs were either counted or, in most cases, measured photometrically in a chromatogram scanner. Grain counts were performed on photographs obtained with 400 to 800-fold magnification, whereas for the scanning 100-fold magnification was used. The slit of the scanner was 1 cm high and 0.1 cm wide; thus, 1 cm broad tracks could be scanned on sections of the photographs. The tracing produced this way gave the distribution of silver grains along the direction of scanning. Thus, the distribution of radioactivity per unit area across a border between two adjacent cell types could be obtained.

Results

The Border between Mutant and Wildtype Liver Cells

Monolayers of normal liver cells (RLB) and the hypoxanthine phosphoribosyl transferase-deficient mutant cells (RLB HPRT^{-}) were placed adjacent to each other as described. This preparation was incubated

with radioactive hypoxanthine for one day and processed for autoradiography. The resulting autoradiographic picture showed heavy labelling over the RLB cells and no labelling above background at the position of the RLB HPRT$^-$ cells. The border between the two monolayers did not show a sudden change in the intensity of labelling, but it decreased gradually over several cell diameters from RLB towards RLB HPRT$^-$.

Photographs taken from such a border region with bright-field and dark-field illumination are shown in Fig. 1*c* and *d*, respectively. The silver grains appear bright in dark-field illumination, and are the only feature seen there. The border between RLB and RLB HPRT$^-$ runs vertical at the position of the arrowhead. Its exact position cannot be given using this pair of cell types, because there are no outstanding morphological differences between single RLB and RLB HPRT$^-$ cells. However, there is a clear border and not an intermixing of labelled and unlabelled cells which would result in a more mottled appearance of the border region. Wild-type cells, for instance would then have been found in the monolayer of RLB HPRT$^-$ at some distance from their own monolayer, and these cells would give rise to islets of stronger labelling. The small spots of stronger labelling in the monolayer of RLB HPRT$^-$ seen in Fig. 1*d* are due to heavier labelling of the nuclei in some of the cells. Although single cells cannot be distinguished unambiguously, it should be noted that the two monolayers do have a somewhat different appearance, and the position of the border can be recognized by a slight orientation parallel to its direction in this region of the otherwise isotropic cells. In addition, the position of the silicone barrier where the border will develop can be marked on the petri dish.

To explore the situation further, one day after joining of the monolayers of the two cell types a scratch was made along their border, scraping away about seven rows of cells (about 200 μm), thus separating the two cell types again. Fig. 1*a* and *b* show an autoradiograph of such a preparation after incubation with ^{3}H-hypoxanthine overnight. Cytochalasin B has been used during the incubation period at a concentration of 4 μg/ml to inhibit cell migration and closure of the gap which would have occurred otherwise during this time. Fig. 1*c* and *d* are from an unscraped border region of the same petri dish and may therefore be compared directly with Fig. 1*a* and *b*.

No single labelled or islets of labelled cells are found in the monolayer of RLB HPRT$^-$ after its separation from RLB. This can be taken as an indication against a broader zone of intermixing of the two cell types.

Now it can be deduced from Fig. 1*b* and *d* that RLB HPRT$^-$ cells

touching RLB wildtype cells show incorporation of radioactivity from ^{3}H-hypoxanthine, which the HPRT$^-$ mutants cannot incorporate when seeded alone or in greater distance from RLB. This is in accordance with the earlier observation (Azarnia *et al.*, 1972), that contact with RLB leads to incorporation of hypoxanthine-derived radioactivity into polyoma transformed BHK 21 cells deficient in inosine pyrophosphorylase (BHK PyY IPP$^-$), and in accordance with the first observation of such an effect between BHK 21 wild-type and BHK PyY IPP$^-$ cells, which has been called metabolic cooperation (Subak-Sharpe *et al.*, 1966).

In the preparation shown in Fig. 1*c* and *d*, RLB HPRT$^-$ cells located some cell diameters away from wild-type RLB cells show incorporation of radioactivity to a lesser degree; this relatively short range of metabolic cooperation has also been observed in previous cell mixing experiments between a single BHK 21 cell and a short row of BHK PyY IPP$^-$ cells connected with it (Subak-Sharpe *et al.*, 1969).

No noticeable increase of grain counts above background can be found in mutant RLB cells more than 2 mm away from the border to wild-type. It cannot be decided for the cells used here whether the nucleotides derived from hypoxanthine, or an activator of hypoxanthine phosphoribosyl transferase, or the enzyme itself is transferred from one cell interior to the next. Cell separation experiments with other cell types seem to rule out the last possibility (Cox *et al.*, 1970; Pitts, 1971). A similar experiment has been performed here. As mentioned above, separating the cell types by a scratch immediately before (1–5 min) addition of radioactive hypoxanthine, prevented the incorporation of any radioactivity into RLB HPRT$^-$. This can be taken as indication against the hypothesis that the enzyme itself is transferred since it is stable in vitro, the reaction measured in the enzyme test (Harris & Cook, 1969) proceeds with the same speed for several hours (U. Friedrich, *personal communication*), and should thus still be present in the RLB HPRT$^-$ cells, unless it is much more unstable in vivo. Not much can be said against the hypothesis that a small activator molecule is transferred from cell to cell, if the maintenance of the concentration of this molecule in the HPRT$^-$ cells were dependent on a continuous supply from the wild-type cells. For HPRT$^-$ mutants in other cell systems, the possibility has been discussed that they arise through regulatory defects rather than through defects in the structural gene for this enzyme (e.g., DeMars, 1974), and this possibility cannot be ruled out for the mutant investigated here. The hypothesis that purine nucleotides derived from hypoxanthine are transferred is compatible with all observations made on metabolic

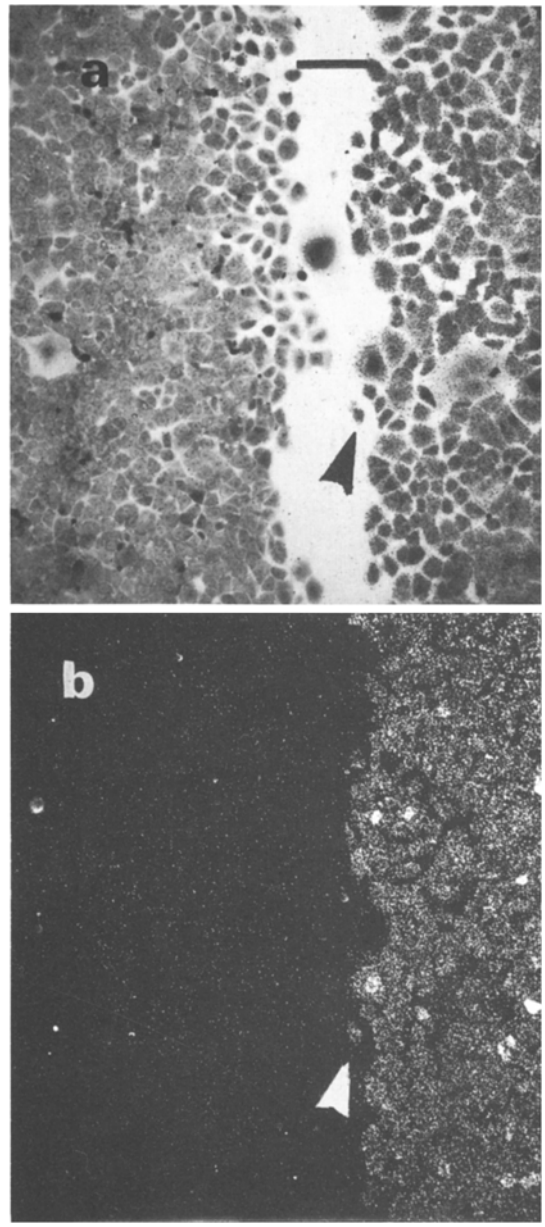

Fig. 1. Autoradiographs from the border between RLB and RLB HPRT$^-$ monolayers. Monolayers of RLB and RLB HPRT$^-$ were placed adjacent to each other as described. One day after first contact between monolayers of different cell type a scratch, about 200 μm broad, was made along their border. Care was taken to scrape away RLB HPRT$^-$ predominantly. It took 1–4 min to scrape a stretch of 1 cm, depending on the discernibility of the border line. Immediately thereafter ^{3}H-hypoxanthine was added as described and

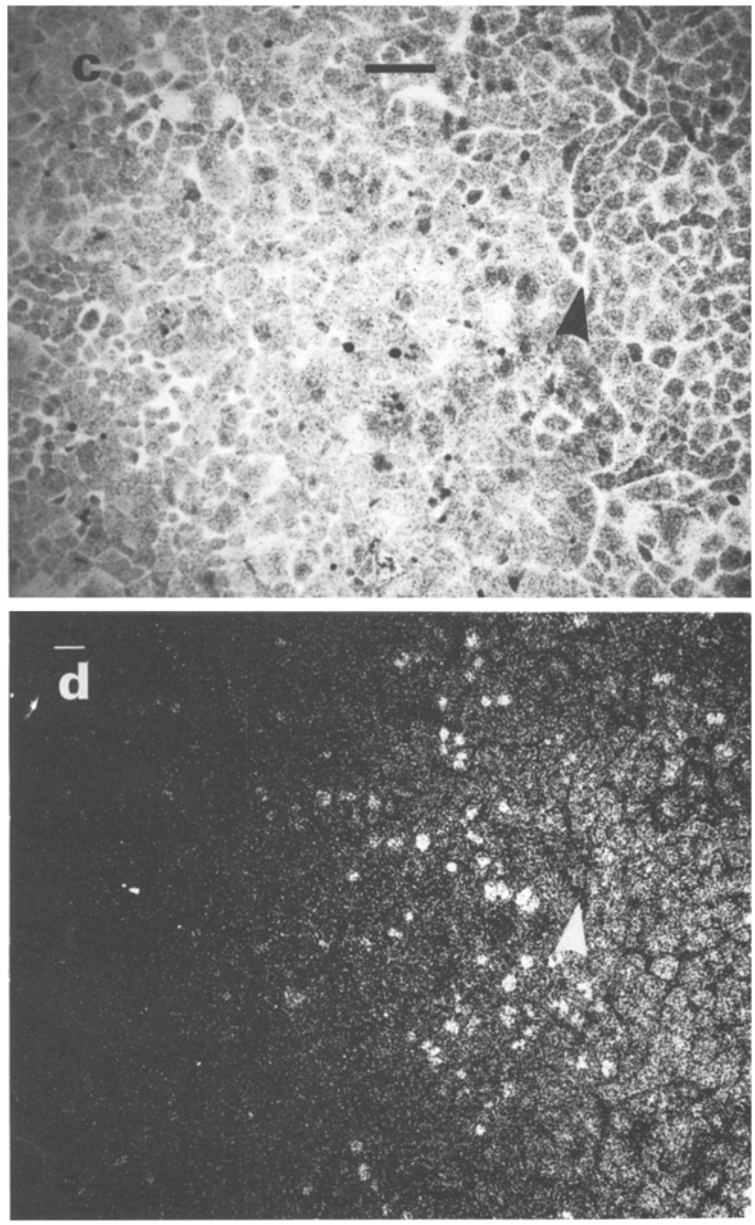

in addition Cytochalasin B (4 μg/ml) was added to reduce cell movement and retard closure of the gap. (*a*) and (*c*) are bright-field pictures of scratched and intact border regions respectively from the same petri dish; (*b*) and (*d*) are dark-field pictures from the same regions. The RLB monolayer is on the right side of the pictures. The black and white arrowheads point to corresponding points; in (*c*) and (*d*) they point to the border which runs about vertical on the pictures. The length of the calibration bar is 100 μm

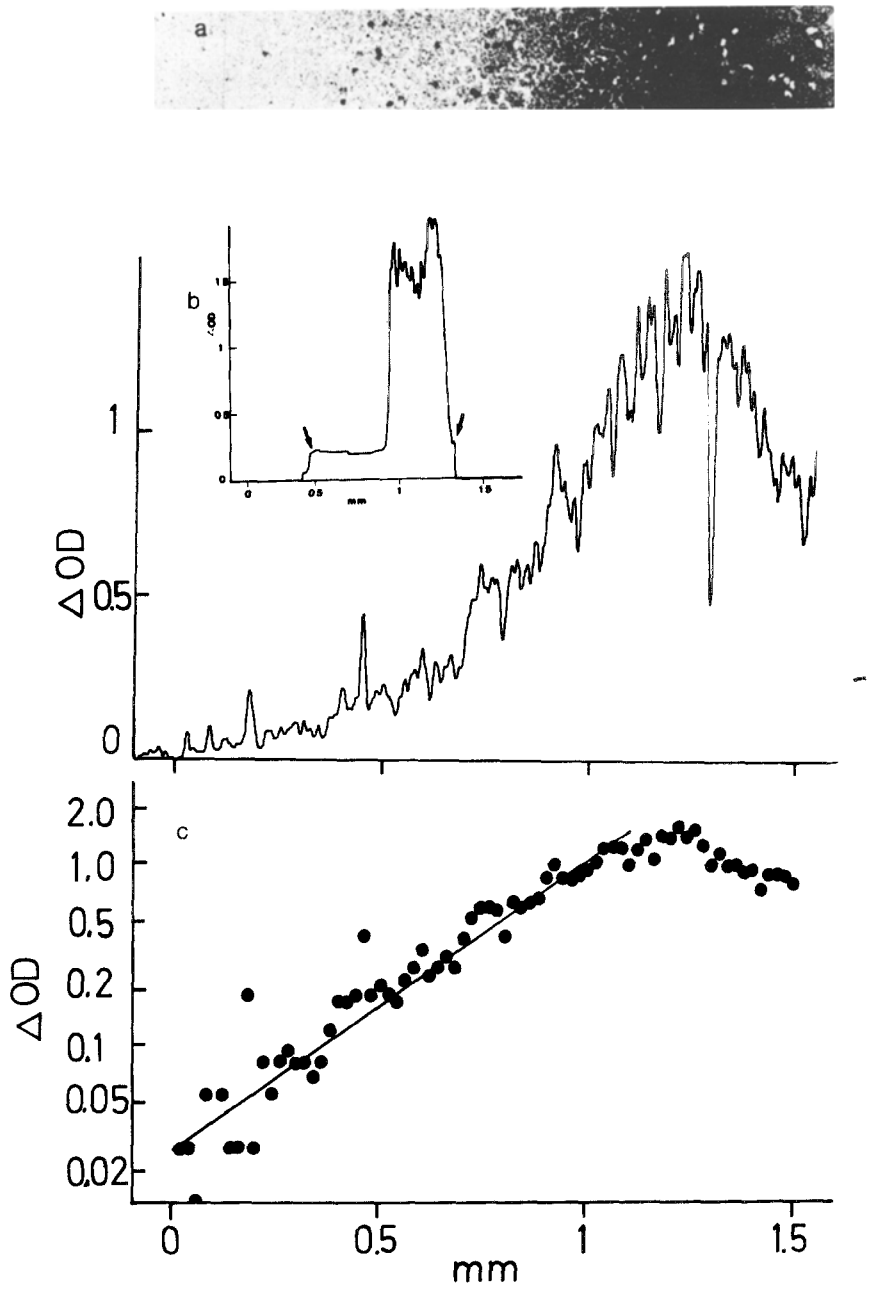

Fig. 2. Distribution of incorporated radioactivity derived from hypoxanthine across the border between RLB and RLB HPRT$^-$ cells. (*a*): Negative of a dark-field picture of an autoradiograph from the border region. (*b*): Tracing of the photometric scan along this negative. (*c*): The lower plateau value of the trace produced by the chromatogram scanner was substracted from the values at different positions of the decreasing part of the trace and plotted *vs.* this position. Under the conditions used an intensity change of 1 OD unit resulted in a 76 mm deflection of the pen of the recorder, as determined with calibrated grey glasses supplied with the instrument. RLB HPRT$^-$ is on the left side, the border to RLB is at 1.2 mm. *Inset:* Tracing produced by scanning along superposed stripes cut from the negative of Fig. 1*b*

cooperation so far, and the following results will be described in terms of this hypothesis, without the implication that it offers the only correct explanation.

The present method of placing a monolayer of one cell type adjacent to another allows a quantitative evaluation of the range of interaction between the two cell types. The segment shown in Fig. 2*a* crosses the main direction of the border between RLB and RLB HPRT$^-$ perpendicularly. The spectrophotometrical scan along this segment (Fig. 2*b*) shows a high optical density at the position of RLB. It has been observed several times, but not always, that the label at the position of the border is even higher than at the position of the HPRT$^+$ cell type, and it appears that in these cases the newly grown cells show more incorporation than the ones which filled the compartments before the plastic obstacle was removed. Progressing into the RLB HPRT$^-$ monolayer, the optical density begins to decline and reaches a plateau of low optical density after several hundred μm. This low optical density was substracted from the higher values at 20 μm intervals (this equals 2 mm on the microphotograph and the recording of the spectrophotometer) and the resulting differences were plotted on a logarithmic scale vs. the distance along the segment. This plot resulted in a straight line which ended in a plateau when apparently the monolayer of RLB was reached (Fig. 2*c*). From the inset in Fig. 2*b*, which shows a trace obtained from the negative of Fig. 1*c*, it can be seen, as already from the photograph itself, that no such gradual decrease of radioactivity is observed when the contact between RLB and RLB HPRT$^-$ is interrupted.

The exponential decrease of radioactivity in the RLB HPRT$^-$ monolayer with increasing distance from the monolayer of RLB can be described by

$$N/N_0 = e^{-kD} \tag{1}$$

where N_0 is the amount of radioactivity incorporated per unit area into RLB at the border, and N the amount per unit area incorporated into RLB HPRT$^-$ at a distance D from the border between the two cell types. The value k describes the steepness of the exponential gradient. In the example presented in Fig. 1, the value of k is 3.7 mm^{-1}, which means that the space constant (the distance along which N/N_0 falls by a factor e^{-1}) is 0.27 mm in this case.

Comparison of Grain Counts and Photometric Scan

Monolayers of RLB and RLB HPRT$^-$ were placed adjacent to each other as described. Six days after first contact ^{3}H-hypoxanthine was

added and a transfer experiment performed as described. Dark-field pictures from the same region of the RLB-HPRT$^-$ monolayer close to the border between the two cell types were taken with 720 and 100-fold magnification. A stripe from the latter was evaluated photometrically while on the corresponding (bigger) stripe obtained with higher magnification the autoradiographic silver grains were counted.

Both measurements gave high values close to the RLB monolayer and decreased with increasing distance from it until they approximated a plateau. As previously, this was taken as background and subtracted from the preceding measurements. The natural logarithms of the differences were plotted *vs.* the distance on the stripe of monolayer from which the pictures were derived (Fig. 3). From there it can be seen that both measurements resulted in almost the same slope for the gradient of radioactivity from the border into the monolayer of RLB HPRT$^-$. The calculated k values [*see* Eq. (1)] were 3.9 ± 0.18 mm^{-1} for the grain count, and 3.5 ± 0.11 mm^{-1} for the photometric scan. Fig. 3 also demonstrates that the photometric method can be used on high grain densities were counting becomes quite impractical. This has been inferred from the fact that, even beyond the point were grain counting was stopped, the optical density of the stripe continued to increase exponentially, i.e., linearly on this semilogarithmic plot, without a sign of saturation up to at least 2 OD. A linear plot of values from the photometric scan *vs.* corresponding grain counts resulted in a straight line and a correlation coefficient of 0.98 was found. So the photometric evaluation of darkfield photographs of autoradiographs seemed justified and was used predominantly. The plots in Fig. 3 from both measurements show deviations from linearity close to the background. It has not been determined if this is due to inaccurate determination of the background, or if it represents a true characteristic of the system.

The Border between RLB HPRT$^-$ and Lens

Similar experiments as described above were performed also with rabbit lens cells as donors of radioactivity, because these could be distinguished unambiguously from RLB HPRT$^-$ and the border between the two cell types could be determined exactly.

Fig. 4 shows that lens cells from rabbit can transfer radioactivity from ^{3}H-hypoxanthine to the HPRT deficient rat liver cells. This confirms electrical measurements which had already demonstrated the possibility

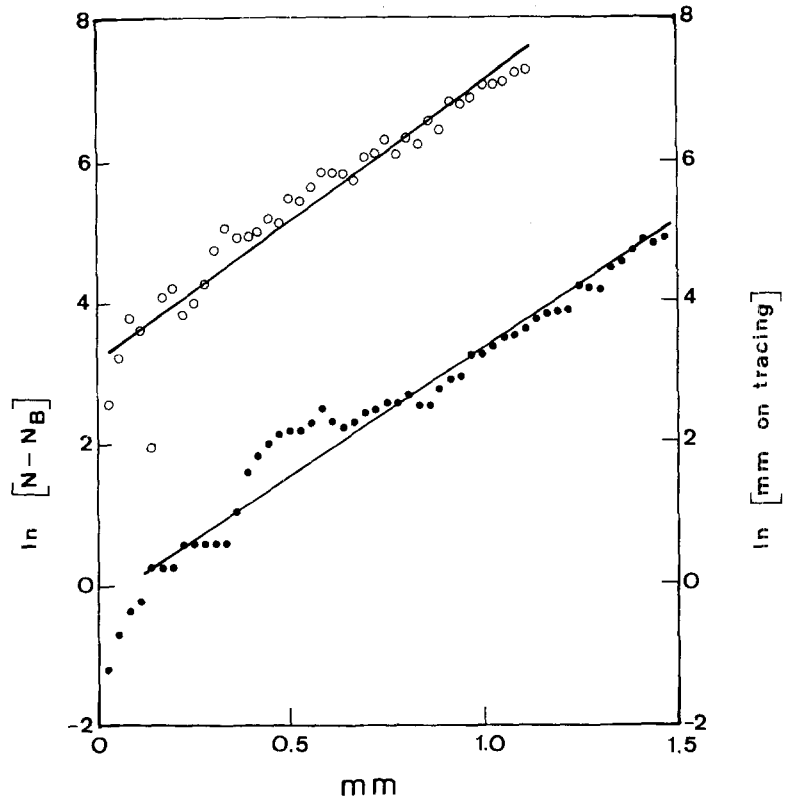

Fig. 3. Comparison of grain count and optical density measurement on a gradient of autoradiographically produced silver grains. Experiments and measurements are described in the text. (*a*) Grain counts: N_B = number of grains in a standard area (27.8× 100 μm) at background labelling intensity in the monolayer of RLB HPRT$^-$. N = number of grains per standard area in the gradient. The natural logarithm of (N–N_B) is plotted *vs.* the position (mm) of the standard area from which N was derived (○). (*b*) Photometric scanning: As in Fig. 2*c*, the optical density values (mm on the tracing produced by the chromatogram scanner; 76 mm represent 1 OD unit) read from the tracing were plotted semilogarithmically (●). The straight lines were calculated with the method of least squares

of exchange of molecules between lens cells and RLB wild type (Michalke & Loewenstein, 1971).

The slope of the radioactivity gradient should be the same as in the previous example if the coupling properties of the cells in the mutant monolayer were not influenced by the adjacent cell type. In fact, the gradient shown in Fig. 4 happens to be steeper than the ones in Figs. 2 and 3, but from the data shown in Table 1 it appears that the mean space constant is the same for gradients starting from either RLB or from lens cells. This means that, using the described methods, no in-

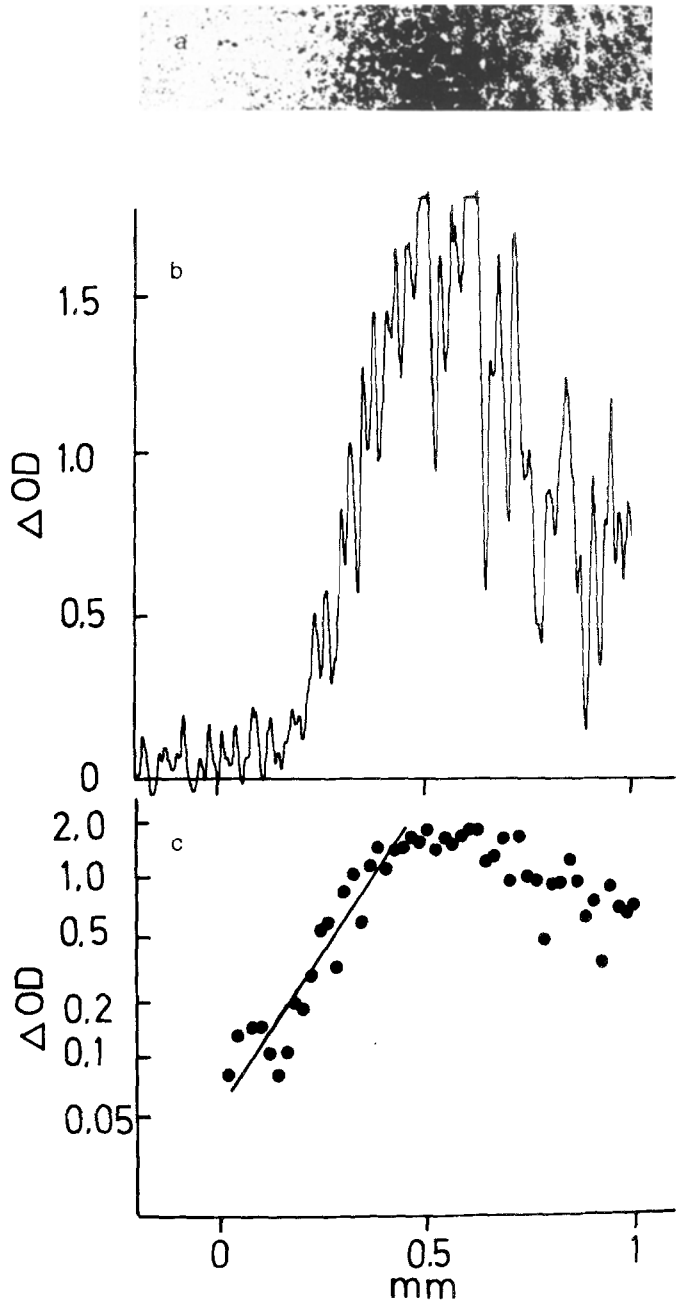

Fig. 4. Distribution of incorporated radioactivity derived from hypoxanthine across the border between lens and RLB HPRT$^-$ cells. (*a*): Negative of a dark-field picture of an autoradiograph from the border region. (*b*): Tracing of the photometric scan along this negative. (*c*): Semilogarithmic plot of points read from the tracing. RLB HPRT$^-$ is on the left side, the border to lens is situated at 0.55 mm

Table 1. Steepness of different gradients in monolayers of RLB HPRT$^-$ cells

Segment No.	Two days after first contact	Four days after first contact	Cell type used as donor of radioactivity	
2	250	90		
3	260	90		
5	150	310	RLB	191 ± 76
6	140	270		(mean and SD)
8	130	230		
9	130	240		
2	160	280		
3	180	280		
5	130	290	lens	191 ± 60
6	160	105		(mean and SD)
8	160	170		
9	200	180		
mean and SD	171 ± 45	211 ± 82		

The values shown in the table are distances (μm) along the exponential part of the gradient over which the labelling intensity falls by a factor e^{-1} (space constant). (SD = standard deviation).

fluence regarding the extent of coupling reaching from lens cells into the RLB HPRT$^-$ monolayers could be detected. If such an influence should exist, its effect on cell to cell communication is masqued by the observed local fluctuations in cell communication.

In the segment shown in Fig. 4, the border between the two cell types is at 0.55 mm. Hence per unit area more radioactivity is incorporated into the RLB HPRT$^-$ cells at the border than into the neighboring lens cells. In this respect Fig. 4 does not show an exceptional example, but such a situation can be found at many places along the border lens to RLB HPRT$^-$, although not everywhere. An example of a larger region can be seen in Fig. 5, which also demonstrates the morphological differences between the two cell types. Fig. 5 is typical in the way that regions of RLB HPRT$^-$ with high incorporation per unit area seem to alternate with regions of less incorporation along the border to the lens cells.

An interesting possibility, to explain the stronger labelling of the HPRT-deficient cells, would be a higher rate of nucleic acid synthesis in these cells. But one still has to consider the more trivial possibility that the RLB HPRT$^-$ cells are just thicker, so below the nuclear track

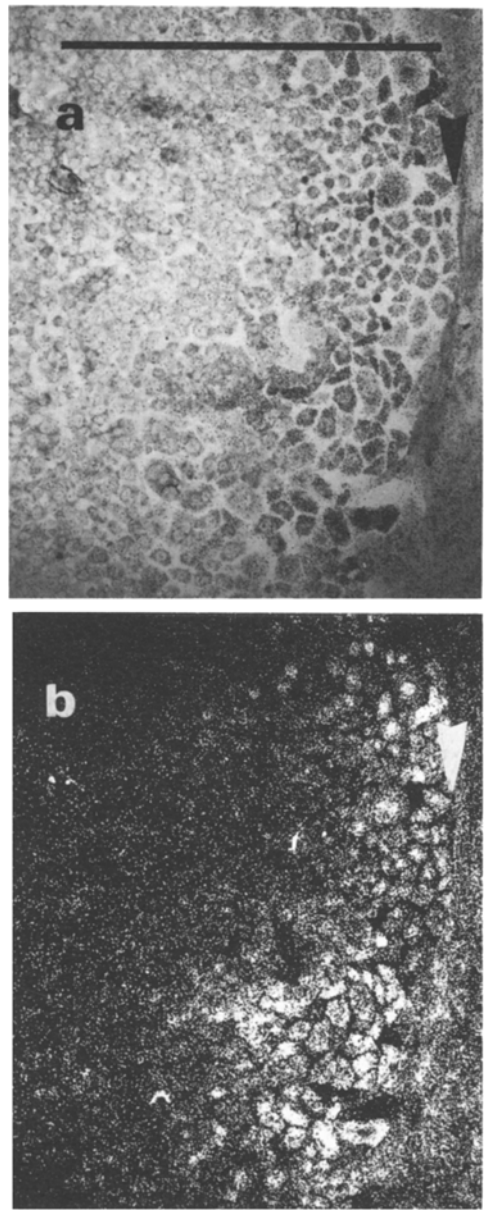

Fig. 5. Distribution of incorporated radioactivity derived from hypoxanthine along the border between lens and RLB HPRT$^-$ cells. (*a*) Bright-field illumination. (*b*) Dark-field illumination. RLB HPRT$^-$ is on the left side. Calibration bar 500 μm

emulsion there is more radioactive material per RLB HPRT$^-$ cell surface, but its concentration per cell volume is not so different; because o the weak energy of the radiation from Tritium this argument woulc

be possible for cell thickness below 2 μm (Sidman, 1970). This argument would imply, however, that the weakly labelled RLB HPRT$^-$ cells are more flat than their more strongly labelled neighbors. No indication for this can be found in the intensity of the Giemsa stain in the respective areas. So the stronger labelling in some areas could indeed be a result of more incorporation of hypoxanthine-derived radioactivity per cell volume, and one would have to assume a higher rate of nucleic acid synthesis in the respective areas of the RLB HPRT$^-$ monolayer, compared to the rate of nucleic acid synthesis in the lens cells.

Gradients in Different Segments of a Monolayer

Table 1 shows space constants of gradients of radioactivity measured in segments on two preparations of different age. On the same dish RLB and lens cells were used to form monolayers of HPRT$^+$ cells, each of which was bordering upon the same monolayer of RLB HPRT$^-$. Two and four days after first contact of the monolayers, transfer experiments were started. Dark-field photographs from both border regions were cut into segments and scanned photometrically. The traces obtained were converted to semilogarithmic plots as described, from which slopes of the gradients and space constants were calculated.

It can be seen from Table 1 that segments from a series, which originate from the same area in a dish, give quite different space constants. The fluctuation is large in the two day as well as in the four day old preparation and occurs on the borders to both HPRT$^+$ cell types. These fluctuations do not appear to be systematic, since the mean values of space constants for gradients starting from the monolayer of RLB or lens are more or less the same, and also the mean values for the two and four day old preparations do not appear significantly different.

Since the determination of the slope of a single segment is not sufficiently inaccurate to explain such large unsystematic fluctuations, it may be concluded that in different segments of a seemingly homogeneous monolayer metabolic cooperation is not equally efficient. It should be mentioned in this connection, however, that even the low space constant of 90 μm (Table 1) could be regarded as substantial metabolic cooperation, since it would mean that 72% of label has been found in a HPRT$^-$ cell neighboring a HPRT$^+$ cell with 100% radioactive label, assuming a cell diameter of 30 μm.

Discussion

Decreasing amounts of radioactivity derived from hypoxanthine are found incorporated into a monolayer of HPRT-deficient rat liver cells with increasing distance from its border to a monolayer of wild-type liver or rabbit lens cells. The gradient of radioactivity thus formed can be described by an exponential function of the form e^{-kD}, where D is the distance from the monolayer of wild-type cells, and k describes the slope of the gradient. Its value is about $5\ mm^{-1}$; i.e., only 0.5% of the radioactivity incorporated into the wild-type cells is found in the $HPRT^-$ cells at 1 mm distance from their border to the wild type.

These gradients can arise the following way. Radioactive purine nucleotides generated from radioactive hypoxanthine in the wild type can reach the $HPRT^-$ cells by intercellular diffusion. There they are progressively diluted by nonradioactive de novo synthesized purine nucleotides. Loss of nucleotides on their way from cell to cell to the outside medium as well as incorporation into nucleic acids both decrease the amount of radioactive material free to diffuse from cell to cell. Thus, nucleotide pools with decreasing specific activity correlated with increasing distance from the wild-type cells are established. Nucleic acids synthesized from these pools in the HPRT deficient cells thus contain decreasing amounts of radioactivity, which leads to the observed autoradiographic pictures. Various factors, like nucleotide pool size, rate of nucleic acid synthesis, and possibly pool expansion as a result of the introduction of hypoxanthine to the outside medium are expected to influence the slope of the gradients, besides the number and quality of the communicative junctions, which are assumed to offer the path for the diffusion of radioactive material from cell to cell (Azarnia *et al.*, 1972; Gilula *et al.*, 1972).

A number of organs and organisms in which such gradients of diffusible substances might be responsible for orderly development have a size on the order of 1 mm (Wolpert, 1969). The concentration of radioactive material in the model gradients described here would change by a factor of about 100 over this distance. This should be well within the sensitivity range of a hypothetical concentration sensor within the cells. If a substance capable of regulating development is generated preferentially at a particular locus in the embryo or tissue, a system of cells connected by communicative junctions can indeed serve as space for diffusion gradients of such substances.

It can be assumed that the first step in the action of a small molecule of the regulation of development is presumably its binding to a macromo-

lecular receptor, which upon binding of the small diffusible ligand changes its activity. This change in activity (supposedly important in a developmental process) depends on the amount of complex formed, which in turn depends on the concentrations of its components and its dissociation constant.

How does the concentration of such a complex change along an exponential concentration gradient of one of its components, i.e., the ligand which can diffuse from one cell interior to the next and build up such a gradient? The following simplefying assumptions are made to explore this question: (1) The total concentration of macromolecular receptor, $[B_0]$, is the same in all cells along the gradient. This molecule cannot diffuse from cell to cell. (2) The dissociation constant K_D is of the same order of magnitude as the concentration of the freely diffusible molecule, $[A]$. The total concentration of free and bound diffusible molecule

$$[A_{tot}]=[A]+[AB] \tag{2}$$

can be higher. For the diffusible molecule a sufficient source is assumed so that $[A_{tot}]$ can always become higher than $[B_0]$. Now the concentration of complex, $[AB]$, can be easily calculated for different concentrations of A along the gradient according to the law of mass action.

$$\frac{[A]\cdot[B]}{[AB]}=K_D. \tag{3}$$

In Fig. 6, for example, the value of K_D has been chosen to be 10^{-5} M, and $[A]$ ranges from 10^{-4} M to 10^{-6} M along the gradient. For the total concentration of macromolecular receptor in the cell, with and without ligand

$$[B_0]=[AB]+[B], \tag{4}$$

three values are chosen arbitrarily (10^{-4} M, 6×10^{-5} M, and 10^{-5} M). Formula (3) and (4) can be combined and rearranged to calculate the concentration of complex, $[AB]$, for any chosen concentration $[A]$ and $[B_0]$.

$$[AB]=\frac{[B_0]}{\left(1+\frac{K_D}{[A]}\right)}. \tag{5}$$

In Fig. 6 over the distance of 1 mm where $[A]$ is assumed to fall

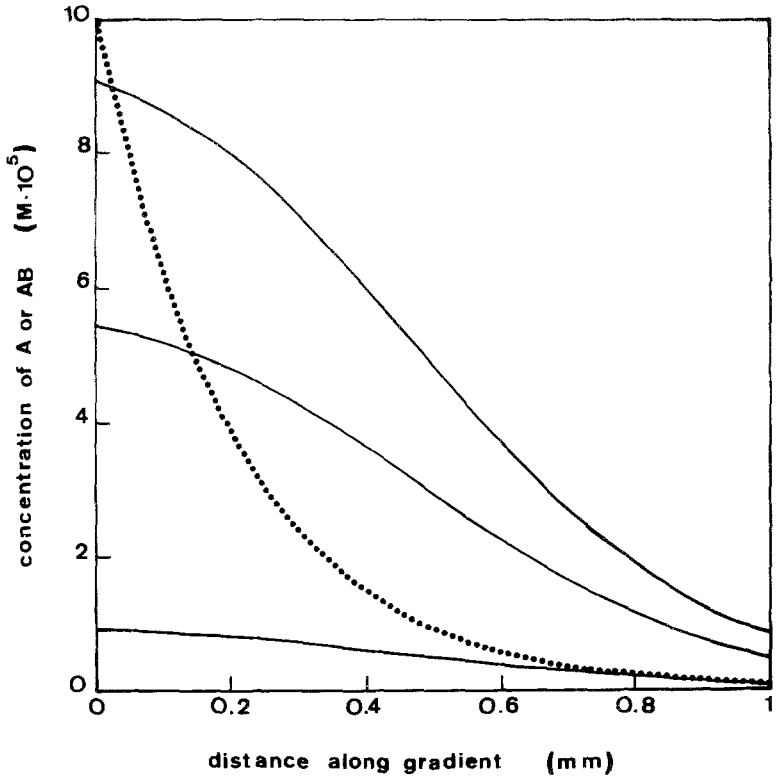

Fig. 6. Concentration change of receptor ligand complex AB along an exponential concentration gradient of ligand A. To construct Fig. 6, $[A]$ (the concentration of A) has been assumed to decrease exponentially from 10^{-4} M to 10^{-6} M over the distance of 1 mm (· · · · ·). The dissociation constant of the complex has been assumed to be 10^{-5} M, which is equal to $[A]$ at 0.5 mm. $[AB]$ is plotted for three arbitrarily selected concentrations of receptor B_0 (10^{-4} M, 6×10^{-5} M, and 10^{-5} M) (——)

exponentially from 10^{-4} M to 10^{-6} M, the calculated $[AB]$ is shown on the same plot. The concentration of complex plotted *vs.* the distance shows a "S"-shaped curve, which approaches linearity when $[A]$ is of the same value as K_D. At the same position where $[A]$ is equal to K_D, the gradient of complex AB is steepest. This position does not depend on $[B_0]$, as long as the supply of diffusible molecule A is not limited. If K_D is changed to 10^{-6} M for example, the steepest part of the gradient of AB will be at the position where $[A]=10^{-6}$ M, i.e., 0.5 mm more distant from the source of A than in Fig. 6.

With different combinations of parameters, e.g., limitations in the supply of A, several interesting situations can be constructed which will

not be discussed here in any detail. Only one more property of a system like this shall be mentioned.

If the concentration $[B_0]$ of receptor molecule is high, compared to $[A]$ and K_D, at any time a substantial amount of ligand will be bound to the receptor and not free to diffuse from cell to cell before dissociation of the complex. In this way it can take much longer, than estimated by taking only free diffusion into account, until a gradient of A and as a consequence of AB becomes stable at its final position. During this time, the steep part of the gradient AB will continue to migrate away from the source of A. Relative slow change of a gradient of positional information has been observed, for example, in transplantation and regeneration experiments with hydra (Wolpert *et al.*, 1972).

These considerations about gradients of diffusible molecules have an appealing corollary concerning the described experiments, as they allow us to construct an argument (although not a very strong one) against the hypothesis that in the presented experiments some activator of the enzyme HPRT, and not the radioactive purine nucleotides themselves, diffuses from cell to cell. This hypothetical activator, assumed to be distributed in an exponential gradient, would have to form a complex with the enzyme HPRT (or something else in the cell) to act. The concentration gradient of this complex is then expected to be reflected by the amount of incorporation of ^{3}H-hypoxanthine into different regions of the monolayer of $HPRT^-$ cells, and this, according to the calculation above, would not result in an exponential decrease of hypoxanthine derived radioactivity with increasing distance from the monolayer of the $HPRT^+$ cells.

I would like to thank J. Campos-Ortega and R. Hertel for persistent encouragement to publish these results and for critical reading of the manuscript. The expert technical assistance of E. Holupirek is gratefully acknowledged. The investigation was financially supported by a grant from the Deutsche Forschungsgemeinschaft.

References

Azarnia, R., Michalke, W., Loewenstein, W.R. 1972. Intercellular communication and tissue growth. VI. Failure of exchange of endogeneous molecules between cancer cells with defective junctions and noncancerous cells. *J. Membrane Biol.* **10**:247

Borek, C., Higashino, S., Loewenstein, W.R. 1969. Intercellular communication and tissue growth. IV. Conductance of membrane junctions of normal and cancerous cells in culture. *J. Membrane Biol.* **1**:274

Child, C.M. 1928. The physiological gradients. *Protoplasma* **5**:447

Cox, R.P., Krauss, M.R., Balis, E.M., Dancis, J. 1970. Evidence for transfer of enzyme product as the basis of metabolic cooperation between tissue culture fibroblasts of Lesch-Nyhan and normal cells. *Proc. Nat. Acad. Sci. USA* **67**:1573

De Mars, R. 1974. Resistance of cultured human fibroblasts and other cells to purine and pyrimidine analogues in relation to mutagenesis detection. *Mut. Res.* **24**:335

Gilula, N.B., Reeves, O.R., Steinbach, A. 1972. Metabolic coupling, ionic coupling and cell contacts. *Nature (London)* **235**:262

Ham, R.G. 1972. Cloning of mammalian cells. *In:* Methods in Cell Physiology. V. Prescott, editor. Academic Press, New York

Harris, H., Cook, P.R. 1969. Synthesis of an enzyme determined by an erythrozyte nucleus in a hybrid cell. *J. Cell Sci.* **5**:121

Lawrence, P.A., Crick, F.H.C., Munro, M. 1972. A gradient of positional information in an insect, Rhodnius. *J. Cell Sci.* **11**:815

Loewenstein, R.R. 1968*a*. Some reflections on growth and differentiation. *Perspect. Biol. Med.* **11**:260

Loewenstein, W.R. 1968*b*. Communication through cell junctions. Implications in growth control and differentiation. *Devel. Biol. Suppl.* **2**:151

Loewenstein, W.R., Kanno, Y. 1964. Studies on an epithelial (gland) cell junction. I. Modification of surface membrane permeability. *J. Cell. Biol.* **22**:565

Loewenstein, W.R., Penn, R.D. 1967. Intercellular communication and tissue growth II. Tissue regeneration. *J. Cell Biol.* **33**:235

Loewenstein, W.R., Socolar, S.J., Higashino, S., Kanno, Y., Davidson, N. 1965. Intercellular communication: Renal, urinary bladder, sensory and salivary gland cells. *Science* **149**:295

Michalke, W., Loewenstein, W.R. 1971. Communication between cells of different type. *Nature (London)* **232**:121

Morgan, T.H. 1905. Polarity considered as a phenomenon of gradation of materials. *J. Exp. Zool.* **2**:495

Penn, R.D. 1966. Ionic communication between liver cells. *J. Cell Biol.* **29**:171

Pitts, J.D. 1971. Molecular exchange and growth control in tissue culture. *In:* Growth Control in Cell Culture. Ciba Foundation Symposion. G.E.W. Wolstenholme and J. Knight, editors. Churchill and Livingstone, London

Shapiro, A.L., Siegel, I.M., Scharff, M.D., Robins, E. 1969. Characteristics of cultured lens cell epithelium. *Invest. Ophthalmol.* **8**:393

Sidman, R.L. 1970. Autoradiographic methods and principles for study of the nervous system with thymidine-H^3. *In:* Contemporary Research Methods in Neuroanatomy. W.J.H. Nauta and S.O.E. Ebbeson, editors. Springer-Verlag, New York

Subak-Sharpe, H., Bürk, R.R., Pitts, J.D. 1966. Metabolic cooperation by cell to cell transfer between genetically marked mammalian cells in culture. *Heredity* **21**:342

Subak-Sharpe, H., Bürk, R.R., Pitts, J.D. 1969. Metabolic cooperation between biochemically marked mammalian cells in tissue culture. *J. Cell Sci.* **4**:353

Wolpert, L. 1969. Positional information and the spatial pattern of cellular differentiation. *J. Theoret. Biol.* **25**:1

Wolpert, L., Clarke, M.R.B., Hornbruch, A. 1972. Positional signalling along hydra. *Nature New Biol.* **239**:101